SAND2018-12651R

Analytic comparison of the dispersion relation of waves present in various MHD models

D. Alcala[1]

[1]New Mexico State Unviersity, Applied Mathematics Department, Las Cruces, New Mexico 88003, USA

(Dated: November 2, 2018)

Ideal magnetohydrodynamics (MHD) has been a widely used theoretical model for studying fusion plasmas. However, as it is well known, MHD is not an entirely accurate physical model and, in some cases, can miss essential physics that is of interest. To remedy this, several improved MHD models have been proposed; these include Hall MHD and a recently developed extended-MHD model [J. W. Burby, Phys. Plasmas **24**, 082104 (2017)]. For these models, it is important to understand the predicted plasma responses to infinitesimal perturbations; that is, their relevant wave dynamics. In this work, I derive the wave dispersion relations for ideal, Hall, and extended MHD models and compare them to those obtained using the two-fluid model for plasmas. It is shown that, for waves with frequencies below or close to the ion gyrofrequency, Hall MHD and extended MHD reproduce quite accurately the wave dispersion relations. However, as it is expected, at higher wave frequencies, all MHD models diverge from the results predicted using the two-fluid model.

I. INTRODUCTION

Ideal magnetohydrodynamics (MHD) can be considered as the bread and butter of plasma fusion research [1], including inertial-confinement-fusion (ICF) plasmas created at Sandia National Laboratories (SNL). However, ideal MHD does not capture a lot of important physics that is of interest in certain experimental regimes. In order to correct for this, several improvements to MHD have been proposed. One particular example is Hall MHD which includes an additional term in Ohm's law. This correction to ideal MHD has led to a better understandin of ICF plasmas, for example, *Hall MHD* is believed to be key to undertanding the origins of the helical instability occuring in the Magnetized Liner Inertial Fusion (MagLIF) experimental platform at SNL [2, 3]. More recently, a new improvement to MHD has been proposed in Ref. [4]. This new model allows for perturbative deviations from exact charge neutrality, as well as perturbative contributions to the transverse electric field and the full effects of finite electron inertia. We shall refer to this model as *extended MHD*.

Before extended MHD can be seriously implemented into a production code, it is important to understand the predicted plasma responses to infinitesimal perturbations; that is, the wave dynamics. In this work, I derive the dispersion relations for ideal, Hall, and extended MHD models. I then compare the dispersion relations to those obtained using the conventional two-fluid model for plasmas. It is shown that, for frequencies below or close to the ion gyrofrequency, Hall MHD and extended MHD reproduce quite accurately the wave dispersion relations. For the parameter regime studied in this work, it seems that Hall MHD reproduces quite accurately the dispersion curves obtained using the more complicated extended-MHD model. However, at higher wave frequencies, both Hall and extended MHD models diverge from the dispersion curves obtained using the two-fluid model.

The present work is organized as follows. In Sec. II, a basic overview is given on wave in plasmas using the well-known two fluid model. In Sec. III, waves in the ideal MHD model are studied. In Sec. IV, the dispersion relations for waves in Hall MHD are obtained. In Sec. V, a brief overview of extended MHD is given and the corresponding wave dispersion relations are discussed. Finally, in Sec. VI, final remarks and conclusions are given.

II. WAVES IN THE TWO-FLUID–MAXWELL SYSTEM

A. Overview

Let us consider the simplified two-fluid–Maxwell system for waves in plasmas. This model will be the base model to compare the dispersion relation of waves for the others MHD models. Our main assumption are the following: (i) collisionless plasma (no friction), (ii) cold plasma (no pressure term), (iii) constant background density and magnetic fields, (iv) no background velocity and electric fields, (v) quasi-neutrality for the background plasma, and (vi) linear waves. With these assumptions, the equations that make up the two-fluid–Maxwell system are the fluid equations

$$\partial_t n_\alpha + \nabla \cdot (n_\alpha \mathbf{v}_\alpha) = 0, \tag{1a}$$

$$m_\alpha \partial_t \mathbf{v}_{\boldsymbol{\alpha}} + m_\alpha (\mathbf{v}_\alpha \cdot \mathbf{v}) \mathbf{v}_\alpha = q_\alpha \mathbf{E} + q_\alpha \mathbf{v}_\alpha \times \frac{\mathbf{B}}{c}, \tag{1b}$$

and Maxwell's equations of electromagnetism

$$\nabla \cdot \mathbf{E} = 4\pi \sum_\alpha q_\alpha n_\alpha, \tag{2a}$$

$$\nabla \cdot \mathbf{B} = 0, \tag{2b}$$

$$\partial_t \mathbf{B} = -c \nabla \times \mathbf{E}, \tag{2c}$$

$$\partial_t \mathbf{E} = c \nabla \times \mathbf{B} - 4\pi \sum_\alpha q_\alpha n_\alpha \mathbf{v}_\alpha. \tag{2d}$$

Sandia National Laboratories is a multimission laboratory managed and operated by National Technology & Engineering Solutions of Sandia, LLC, a wholly owned subsidiary of Honeywell International Inc., for the U.S. Department of Energy's National Nuclear Security Administration under contract DE-NA0003525.

Here n_α and $\mathbf{v}_\alpha$ denote the number density and velocity field for each species α. The charge and mass are denoted by q_α and m_α, respectively. Also, $\mathbf{E}$ and $\mathbf{B}$ are the electric and magnetic fields, respectively. Finally c is the speed of light.

B. Linearized equations

We linearize Eqs. (1) and (2) by considering a small perturbation about the equilibrium state:

$$n_\alpha = n_{0\alpha} + \epsilon\,\widetilde{n}_\alpha, \tag{3a}$$
$$\mathbf{v}_\alpha = \epsilon\,\widetilde{\mathbf{v}}_\alpha, \tag{3b}$$
$$\mathbf{E} = \epsilon\,\widetilde{\mathbf{E}}, \tag{3c}$$
$$\mathbf{B} = \mathbf{B}_0 + \epsilon\,\widetilde{\mathbf{B}}. \tag{3d}$$

Substituting Eqs. (3) into Eqs. (1) and taking the limit of small ϵ leads to the linearized fluid equations

$$\partial_t \widetilde{n}_\alpha + n_{0\alpha}(\boldsymbol{\nabla}\cdot\widetilde{\mathbf{v}}_\alpha), \tag{4a}$$
$$m_\alpha \partial_t \widetilde{\mathbf{v}}_\alpha = q_\alpha \widetilde{E} + q_\alpha \widetilde{\mathbf{v}}_\alpha \times \mathbf{B}_0/c. \tag{4b}$$

Also, substituting Eqs. (3) into Eqs. (2) and taking the limit of small ϵ leads to the linearized Maxwell equations

$$\boldsymbol{\nabla}\cdot\widetilde{\mathbf{E}} = 4\pi \sum q_\alpha \widetilde{n}_\alpha, \tag{5a}$$
$$\boldsymbol{\nabla}\cdot\widetilde{\mathbf{B}} = 0, \tag{5b}$$
$$\partial_t \widetilde{\mathbf{B}} = -c\boldsymbol{\nabla}\times\widetilde{\mathbf{E}}, \tag{5c}$$
$$\partial_t \widetilde{\mathbf{E}} = c\boldsymbol{\nabla}\times\widetilde{\mathbf{B}} - 4\pi \sum_\alpha q_\alpha \widetilde{\mathbf{v}}_\alpha n_{0\alpha}. \tag{5d}$$

For a given dynamical field $\widetilde{g}$, we propose an ansatz based on the Fourier transform so that $\widetilde{g} = \widehat{g} e^{i\omega t - i\mathbf{k}\cdot\mathbf{x}}$. Then, Eqs. (4) are written as

$$\omega \widehat{n}_\alpha - n_{0\alpha}(\mathbf{k}\cdot\widehat{\mathbf{v}}_\alpha) = 0, \tag{6a}$$
$$i\omega m_\alpha \widehat{\mathbf{v}}_\alpha = q_\alpha \widehat{\mathbf{E}} + q_\alpha \widehat{\mathbf{v}}_\alpha \times \mathbf{B}_0. \tag{6b}$$

Similarly, Eqs. (5) are written as

$$-i\mathbf{k}\cdot\widehat{\mathbf{E}} = 4\pi \sum_\alpha q_\alpha \widehat{n}_\alpha \tag{7a}$$
$$-i\mathbf{k}\cdot\widehat{\mathbf{B}} = 0 \tag{7b}$$
$$\omega\widehat{\mathbf{B}} = c\mathbf{k}\times\widehat{\mathbf{E}} \tag{7c}$$
$$\omega\widehat{\mathbf{E}} = -c\mathbf{k}\times\widehat{\mathbf{B}} - i4\pi \sum_\alpha q_\alpha n_{0\alpha} \widehat{\mathbf{v}}_\alpha. \tag{7d}$$

C. Dispersion relation

Now, let us obtain the eigenvalue equation for the electric field $\widehat{\mathbf{E}}$. First, let's consider momentum equation (6b)

$$i\omega m_\alpha \widehat{\mathbf{v}}_\alpha = q_\alpha \widehat{\mathbf{E}} + q_\alpha \widehat{\mathbf{v}}_\alpha \times \mathbf{B}_0. \tag{8}$$

Solving for $\widehat{\mathbf{v}}_\alpha$, we obtain

$$\widehat{\mathbf{v}}_\alpha = \frac{q_\alpha}{m_\alpha} \boldsymbol{M}\cdot\widehat{\mathbf{E}}, \tag{9}$$

where

$$\boldsymbol{M} \doteq \begin{pmatrix} \frac{i\omega}{(\Omega_\alpha^2-\omega^2)} & \frac{-\Omega_\alpha}{(\Omega_\alpha^2-\omega^2)} & 0 \\ \frac{-\Omega_\alpha}{(\Omega_\alpha^2-\omega^2)} & \frac{i\omega}{(\Omega_\alpha^2-\omega^2)} & 0 \\ 0 & 0 & -\frac{i}{\omega}, \end{pmatrix} \tag{10}$$

where Ω_α is the gyrofrequency of α:

$$\Omega_\alpha \doteq \frac{q_\alpha B_0}{m_\alpha c}. \tag{11}$$

Substituting $\widehat{\mathbf{B}} = c\mathbf{k}\times\hat{\mathbf{E}}/\omega$ and $\widehat{\mathbf{v}}_\alpha$ into Eq. (7d) leads to the following eigenvalue equation for $\widehat{\mathbf{E}}$:

$$\begin{pmatrix} S - n^2\cos^2(\theta) & -iD & n^2\cos(\theta)\sin(\theta) \\ iD & S-n^2 & 0 \\ n^2\cos(\theta)\sin(\theta) & 0 & P - n^2\sin^2(\theta) \end{pmatrix} \begin{pmatrix} \hat{E}_x \\ \hat{E}_y \\ \hat{E}_z \end{pmatrix} = \mathbf{0}, \tag{12}$$

The condition for a nontrivial solution of the vector wave equation is that the determinant of the dispersion matrix be zero. This condition gives the dispersion relation $D(\omega,\mathbf{k})$, which in principle, can be inverted in order to determine the wave frequency ω as a function of the wave vector $\mathbf{k}$: $\omega = \omega(\mathbf{k})$. Setting the determinant of the above matrix to zero yields

$$An^4 - Bn^2 + C = 0, \tag{13}$$

where $n \doteq ck/\omega$ is the refraction index and

$$A \doteq S\,\sin^2(\theta) + P\,\cos^2(\theta), \tag{14a}$$
$$B \doteq RL\,\sin^2(\theta) + PS\,[1+\cos^2(\theta)], \tag{14b}$$
$$C \doteq PRL, \tag{14c}$$
$$S \doteq (R+L)/2, \tag{14d}$$
$$D \doteq (R-L)/2, \tag{14e}$$
$$R \doteq 1 - \sum_\alpha \frac{\omega_\alpha^2}{\omega(\omega+\Omega_\alpha)}, \tag{14f}$$
$$L \doteq 1 - \sum_\alpha \frac{\omega_\alpha^2}{\omega(\omega-\Omega_\alpha)}. \tag{14g}$$

Here ω_α is the plasma frequency of the species α:

$$\omega_\alpha \doteq \sqrt{\frac{4\pi n_{0\alpha} q_\alpha^2}{m_\alpha}}. \tag{15}$$

The solution to Eqs. (13) is trivial:

$$n^2 = \frac{B}{2A} \pm \frac{\sqrt{B^2-4AC}}{2A}. \tag{16}$$

In the following sections, we shall compare this solution with those obtained using various MHD models.

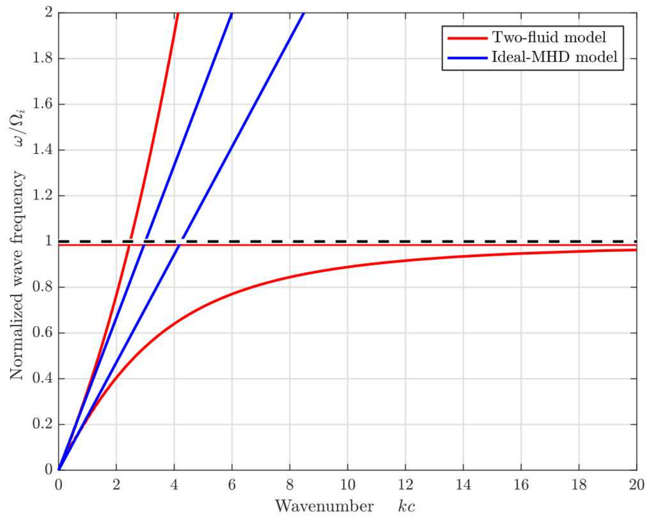

FIG. 1: Comparison of the normalized wave frequency ω/Ω_i using the ideal-MHD and the two-fluid models. In this work, we used as dimensionless parameters $|\omega_{pe}/\Omega_e| = 3$ and $|\Omega_e/\Omega_i| = 100$, which led to a normalized Alfven speed of $v_a/c \simeq 3/100$. The propagation angle considered is $\theta = \pi/4$.

III. WAVES IN THE IDEAL MHD MODEL

A. Overview

In MHD, the plasma is considered as a perfectly conducting, single component fluid. The governing equations of MHD are given by

$$\partial_t \rho + \boldsymbol{\nabla} \cdot (\rho \mathbf{v}) = 0, \tag{17a}$$
$$\rho \partial_t \mathbf{v} + \rho(\mathbf{v} \cdot \boldsymbol{\nabla})\mathbf{v} = \mathbf{J} \times \mathbf{B}, \tag{17b}$$
$$\partial_t \mathbf{B} = -c\boldsymbol{\nabla} \times \mathbf{E}, \tag{17c}$$

where $\rho \simeq n_i m_i$ is the ion mass density and $\mathbf{v} \simeq \mathbf{v}_i$ is the ion velocity field. In ideal MHD, the current $\mathbf{J}$ is determined by neglecting the displacement current, *i.e.*, the $\partial_t \mathbf{E}$ term, in Ampère's equation (2d)

$$c\boldsymbol{\nabla} \times \mathbf{B} = 4\pi \mathbf{J}. \tag{18}$$

The electric field $\mathbf{E}$ is determined using the ideal Ohm's law

$$\mathbf{E} = -\mathbf{v} \times \mathbf{B}/c. \tag{19}$$

The well-known MHD equations are obtained when inserting Eqs. (18) and (19) into Eqs. (17):

$$\partial_t \rho + \boldsymbol{\nabla} \cdot (\rho \mathbf{v}) = 0, \tag{20a}$$
$$\rho \partial_t \mathbf{v} + \rho(\mathbf{v} \cdot \boldsymbol{\nabla})\mathbf{v} = c\,(\boldsymbol{\nabla} \times \mathbf{B}) \times \mathbf{B}/(4\pi) \tag{20b}$$
$$\partial_t \mathbf{B} = \boldsymbol{\nabla} \times (\mathbf{v} \times \mathbf{B}). \tag{20c}$$

As noted before, here we shall neglect the plasma thermal pressure in Eq. (20b).

B. Linearized equations

We linearize Eqs. (20) by considering a small perturbation about the equilibrium state:

$$\rho = \rho_0 + \epsilon\, \widetilde{\rho}, \tag{21a}$$
$$\mathbf{v} = \epsilon\, \widetilde{\mathbf{v}}, \tag{21b}$$
$$\mathbf{B} = \mathbf{B}_0 + \epsilon\, \widetilde{\mathbf{B}}. \tag{21c}$$

Substituting Eqs. (21) into Eqs. (20) and taking the limit of small ϵ leads to the linearized ideal MHD equations:

$$\partial_t \widetilde{\rho} + \boldsymbol{\nabla} \cdot (\rho_0 \widetilde{\mathbf{v}}) = 0, \tag{22a}$$
$$\rho_0 \partial_t \widetilde{\mathbf{v}} = c(\boldsymbol{\nabla} \times \widetilde{\mathbf{B}}) \times \mathbf{B}_0/(4\pi), \tag{22b}$$
$$\partial_t \widetilde{\mathbf{B}} = \boldsymbol{\nabla} \times (\widetilde{\mathbf{v}} \times \mathbf{B}_0). \tag{22c}$$

We then Fourier transform the fields so that, for any arbitrary field $\widetilde{g}$, one write $\widetilde{g} = \hat{g}\exp(i\omega t - i\mathbf{k}\cdot\mathbf{x})$. Then, Eqs. (22) become

$$\omega\hat{\rho} - \rho_0 \mathbf{k} \cdot \hat{\mathbf{v}} = 0, \tag{23a}$$
$$\omega\rho_0 \hat{\mathbf{v}} = c\mathbf{B}_0 \times (\mathbf{k} \times \hat{\mathbf{B}})/(4\pi), \tag{23b}$$
$$\omega\hat{\mathbf{B}} + \mathbf{k} \times (\hat{\mathbf{v}} \times \mathbf{B}_0) = 0. \tag{23c}$$

Solving for the magnetic field leads to

$$\omega^2 \widehat{\mathbf{B}} + \frac{c}{4\pi\rho_0}\left[(\mathbf{B}_0 \cdot \mathbf{k})(\mathbf{B}_0 \cdot \widehat{\mathbf{B}})\,\mathbf{k} - (\mathbf{B}_0 \cdot \mathbf{k})^2 \widehat{\mathbf{B}}\right] = \frac{c}{4\pi\rho_0}\left[\mathbf{k}\,(\mathbf{k} \cdot \mathbf{B}_0) - \mathbf{k}^2\, \widehat{\mathbf{B}}_0\right](\mathbf{B}_0 \cdot \widehat{\mathbf{B}}). \tag{24}$$

C. Dispersion relation

Let us consider the case where the background magnetic field is parallel to the z axis so that $\mathbf{B}_0 = B_0 \mathbf{e}_z$. We shall also consider the wavevector $\mathbf{k}$ to lie on the xz plane. Hence, we write $\mathbf{k} = k_x \mathbf{e}_x + k_z \mathbf{e}_z$, where $k_x = k\sin(\theta)$, $k_z = k\cos(\theta)$, and θ is the angle between the wavevector and the background magnetic field. Using this convention, we obtain the following eivenvalue equation:

$$\begin{pmatrix} \omega^2 - k^2 v_A^2 & 0 & v_A^2 k_x k_z \\ 0 & \omega^2 - k_z^2 v_A^2 & 0 \\ v_A^2 k_x k_z & 0 & \omega^2 - v_A^2 k_x^2 \end{pmatrix} \begin{pmatrix} \hat{B}_x \\ \hat{B}_y \\ \hat{B}_z \end{pmatrix} = \mathbf{0}, \tag{25}$$

where

$$v_A = \sqrt{\frac{B_0^2 c}{4\pi\rho_0}} \tag{26}$$

is the Alfven speed. The condition for a nontrivial solution of the vector wave equation is that the determinant of the dispersion matrix in Eq. (25) be zero. This condition gives the dispersion relation

$$\omega^2(\omega^2 - k^2 v_A^2)\left[\omega^2 - k^2 v_A^2 \cos^2(\theta)\right] = 0. \tag{27}$$

There are three independent roots to the above dispersion relation. Note that one of the roots corresponds to $\omega = 0$, which is not a temporally oscillating wave mode. In ideal MHD with the pressure term included, this mode corresponds to the *slow wave*. In ideal MHD with no pressure, the slow wave ceases to exist, so there are only two oscillating wave modes. For the first root, one has

$$\omega = k v_A. \tag{28}$$

This mode is the *compressional Alfven wave*. It corresponds to the fast magnetosonic wave when the pressure term is included. For the second mode, we obtain

$$\omega = k v_A \cos(\theta), \tag{29}$$

which corresponds to the *shear Alfven wave*.

D. Comparison with two-fluid model

Now, let us compare the obtained ideal MHD waves with the waves in the two-fluid model. In Fig. 1, I show ω as a function of $\mathbf{k}$. It can be seen that, at very low wave frequencies (compared to the ion gyrofrequency), the wave frequencies for the ideal-MHD model and the two-fluid model are quite similar. Both models show linear relationships as $k \to 0$. However, as the frequencies grows comparable to the ion gyrofrequency, one sees that the two models diverge.

IV. WAVES IN THE HALL-MHD MODEL

A. Overview

Now, we shall analyze the waves present in the Hall-MHD model. In Hall-MHD, Eqs. (17) and (18) remain the same. However, a corrective term is added to Ohm's law so that

$$\mathbf{E} + \frac{\mathbf{v} \times \mathbf{B}}{c} = \frac{\mathbf{J} \times \mathbf{B}}{q_e n_e}. \tag{30}$$

Using the quasineutrality condition $q_e n_e \simeq q_i n_i$ and substituting Eq. (30) into Eqs. (17) and (18) leads to the Hall-MHD equations

$$\partial_t \rho + \boldsymbol{\nabla} \cdot (\rho \mathbf{v}) = 0, \tag{31a}$$

$$\rho \partial_t \mathbf{v} + \rho(\mathbf{v} \cdot \boldsymbol{\nabla})\mathbf{v} = \frac{c}{4\pi}(\boldsymbol{\nabla} \times \mathbf{B}) \times \mathbf{B}, \tag{31b}$$

$$\partial_t \mathbf{B} = \boldsymbol{\nabla} \times (\mathbf{v} \times \mathbf{B}) + \frac{m_i c}{4\pi q_i \rho} \boldsymbol{\nabla} \times \left[\mathbf{B} \times (\boldsymbol{\nabla} \times \mathbf{B})\right]. \tag{31c}$$

It should be noted that the only difference between the Ideal MHD model and Hall MHD model is the last term in Eq. (31c), which is commonly referred as the "Hall-current term."

B. Linearized equations

As in Eqs. (22), we now linearize the Hall MHD equations by considering a small perturbation about the equilibrium state. Following the same procedure as in Sec. III B, we obtain the linearized Hall-MHD equations:

$$\partial_t \widetilde{\rho} + \boldsymbol{\nabla} \cdot (\rho_0 \widetilde{\mathbf{v}}) = 0, \tag{32a}$$

$$\rho_0 \partial_t \widetilde{\mathbf{v}} = \frac{c}{4\pi}(\boldsymbol{\nabla} \times \widetilde{\mathbf{B}}) \times \mathbf{B}_0, \tag{32b}$$

$$\partial_t \widetilde{\mathbf{B}} = \boldsymbol{\nabla} \times (\widetilde{\mathbf{v}} \times \mathbf{B}_0) - \frac{m_i c}{4\pi q_i \rho_0} \boldsymbol{\nabla} \times [(\boldsymbol{\nabla} \times \widetilde{\mathbf{B}}) \times \mathbf{B}_0]. \tag{32c}$$

As in Sec. III B, we propose the Fourier ansatz for the fields. Then, we obtain the following equations:

$$\widehat{\rho}\omega - \rho_0 \widehat{\mathbf{v}} \mathbf{k} \cdot \mathbf{v}, \tag{33a}$$

$$\omega \rho_0 \widehat{\mathbf{v}} - \frac{c}{4\pi} \mathbf{B}_0 \times (\mathbf{k} \times \widehat{\mathbf{B}}) = 0, \tag{33b}$$

$$\omega \widehat{\mathbf{B}} + \mathbf{k} \times (\widehat{\mathbf{v}} \times \mathbf{B}_0) + \frac{m_i c}{4\pi q_i \rho_0} \mathbf{k} \times \left[\mathbf{B}_0 \times (\mathbf{k} \times \widehat{\mathbf{B}})\right] = 0. \tag{33c}$$

C. Dispersion relation

We use Eq. (33b) to solve for $\widehat{\mathbf{v}}$ so that

$$\widehat{\mathbf{v}} = \frac{c\mathbf{k}\,(\mathbf{B}_0 \cdot \widehat{\mathbf{B}}) - \widehat{\mathbf{B}}\,(\mathbf{B}_0 \cdot \mathbf{k})}{4\pi\omega\rho_0}. \tag{34}$$

Upon inserting $\widehat{\mathbf{v}}$ into Eq. (33c) and adopting the same convention for the background magnetic field and the wave vector $\mathbf{k}$, we obtain an eigenvalue equation for the magnetic field, which is given by

$$\begin{pmatrix} \omega^2 - v_A^2 k_z^2 & -i\frac{\omega}{\Omega_i} v_A^2 k_z^2 & v_A^2 k_x k_z \\ i\frac{\omega}{\Omega_i} v_A^2 k_z^2 & \omega^2 - v_A^2 k_z^2 & -i\frac{\omega}{\Omega_i} v_A^2 k_x k_z \\ v_A^2 k_x k_z & i\frac{\omega}{\Omega_i} v_A^2 k_x k_z & \omega^2 - v_A^2 k_x^2 \end{pmatrix} \begin{pmatrix} \hat{B}_x \\ \hat{B}_y \\ \hat{B}_z \end{pmatrix} = \mathbf{0}, \tag{35}$$

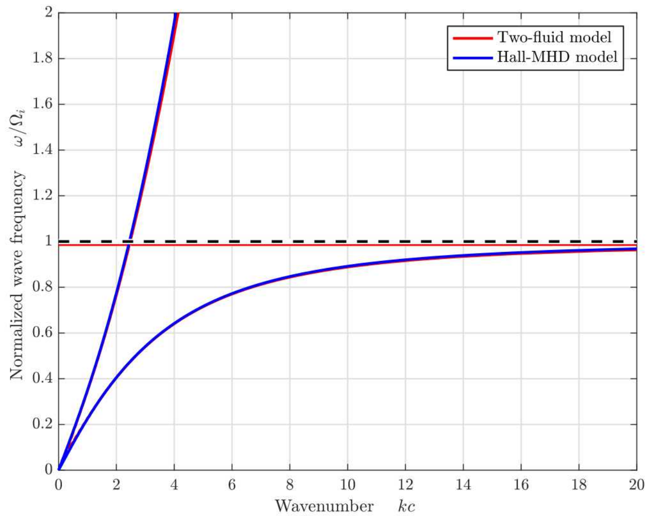

FIG. 2: Comparison of the normalized wave frequency ω/Ω_i using the Hall-MHD and the two-fluid models. Good agreement is obtained for the shear Alfven wave.

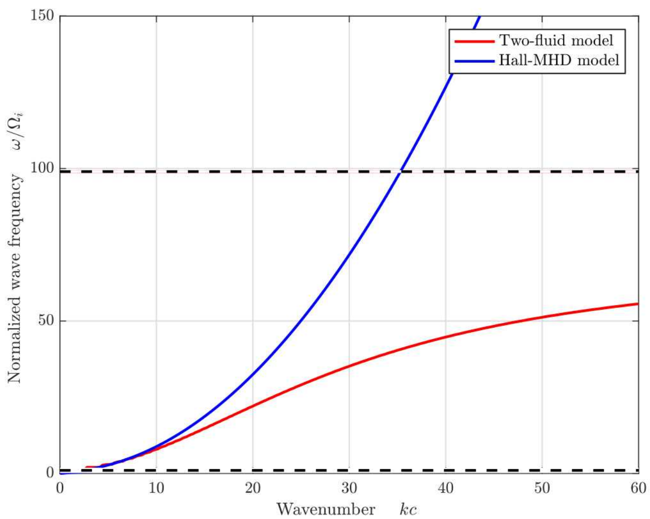

FIG. 3: Comparison of the normalized wave frequency ω/Ω_i using the Hall-MHD and the two-fluid models. As expected the dispersion curves for the two models eventually diverge at large kc.

Note that the matrix in Eq. (35) is similar to that obtained using the ideal-MHD model [see Eq. (25)]. In fact, the only difference resides on the terms that are proportional to ω/Ω_i. It is worth mentioning that MHD, as well as Hall MHD, deals with plasma dynamics that evolves at a time scale much slower than the ion gyro-frequency. In particular, the frequency involved in MHD waves is small compared to the ion gyro-frequency:

$$\frac{\omega}{\Omega_i} \ll 1. \tag{36}$$

Hence, the terms proportional to ω/Ω_i in Eq. (35) should be considered as perturbations only.

Let us now obtain wave frequencies. Calculating the determinant of the dispersion matrix and setting it to zero leads to the dispersion relation for Hall-MHD:

$$\omega^2 \left[(\omega^2 - v_A^2 k^2)(\omega^2 - v_A^2 k_z^2) - \frac{\omega^2}{\Omega_i^2} v_A^4 k_z^2 k^2 \right] = 0. \tag{37}$$

As in ideal MHD, one mode is given by $\omega = 0$, which does not represent an oscillating wave. Also, note that, in the limit $\omega/\Omega_i \to 0$, one recovers the ideal-MHD dispersion relation (27). One can directly solve for the wave frequency. A simple calculation leads to

$$\begin{aligned} \omega^2 = &\frac{1}{2}\left(v_A^2 k^2 + v_A^2 k_z^2 + \frac{v_A^4 k^2 k_z^2}{\Omega_i^2} \right) \\ &\pm \frac{1}{2}\sqrt{\left(v_A^2 k_z^2 + v_A^2 k^2 + \frac{v_A^4 k^2 k_z^2}{\Omega_i^2} \right)^2 - 4 v_A^4 k^2 k_z^2}. \end{aligned} \tag{38}$$

In Eq. (38), the positive and negative roots correspond to the compressional Alfven wave and the shear Alfven wave, respectively.

D. Comparison with two-fluid model

Now, let us compare the obtained Hall-MHD waves with the waves in the two-fluid model. Figure 2 shows ω as a function of $\mathbf{k}$. One can see that Hall MHD does a much better job in obtaining the dispersion relation for the shear Alfven wave. In fact, it is quite surprising that the two models agree quite well for this wave branch in the limit when $\omega \sim \Omega_i$.

Regarding the compressional Alfven wave, as shown in Fig. 2, Hall MHD seems to reproduce quite well the dispersion relation for the compressional Alfven wave upto $\omega \sim 2\Omega_i$. This is surprising because it is expected that Hall MHD is no longer valid for wave frequencies close to or larger than the ion gyrofrequency. However, as shown in Fig. 3, the two Hall-MHD and the two-fluid models eventually diverge at higher frequencies in the regime close to the whistler waves.

V. WAVES IN THE EXTENDED-MHD MODEL

A. Overview

Recently, an extended-MHD model was proposed that allows for perturbative deviations from exact charge neutrality, as well as perturbative contributions to the transverse electric field and the full effects of finite electron inertia [4]. This model can be interpreted geometrically as an invariant slow manifold in the infinite-dimensional two-fluid–Maxwell phase space. Interestingly, a Hamiltonian structure was deduced for the model, which allowed to identify the governing Hamiltonian of the system, as well as the associated Poisson bracket. For more details, see Ref. [4].

In this extended-MHD model, the governing equations for the $(\rho, \mathbf{v}, \mathbf{B})$ fields are given by

$$\frac{\partial \rho}{\partial t} = -\boldsymbol{\nabla} \cdot \left(\frac{\delta \mathcal{H}}{\delta \mathbf{v}}\right), \tag{39a}$$

$$\frac{\partial \mathbf{v}}{\partial t} = -\boldsymbol{\nabla}\left(\frac{\delta \mathcal{H}}{\delta \rho}\right) + \frac{1}{\rho}\left(\boldsymbol{\nabla} \times \frac{\delta \mathcal{H}}{\delta \mathbf{B}}\right) \times \mathbf{B} + \frac{1}{\rho}\frac{\delta \mathcal{H}}{\delta \mathbf{v}} \times (\boldsymbol{\nabla} \times \mathbf{v}), \tag{39b}$$

$$\frac{\partial \mathbf{B}}{\partial t} = -\boldsymbol{\nabla} \times \left(\frac{1}{\rho}\mathbf{B} \times \frac{\delta \mathcal{H}}{\delta \mathbf{v}}\right) - \left(\frac{|\mathbf{B}|}{\Omega_i} - \frac{|\mathbf{B}|}{\Omega_e}\right) \boldsymbol{\nabla} \times \left[\frac{1}{\rho}\left(\boldsymbol{\nabla} \times \frac{\delta \mathcal{H}}{\delta \mathbf{B}}\right) \times \mathbf{B}\right] + \nu Z_i \frac{|\mathbf{B}|^2}{\Omega_i^2} \boldsymbol{\nabla} \times \left[\left(\boldsymbol{\nabla} \times \frac{\delta \mathcal{H}}{\delta \mathbf{v}}\right) \times \frac{1}{\rho}(\boldsymbol{\nabla} \times \mathbf{v})\right], \tag{39c}$$

where $\nu \doteq m_e/m_i$ is the electron to ion mass ratio and $Z_i \doteq -q_i/q_e$. Also, the Hamiltonian $\mathcal{H}$ is defined as

$$\mathcal{H} \doteq \frac{1}{2} \int \mathrm{d}^3\mathbf{x} \left[\rho\,|\mathbf{v}|^2 + \frac{|\mathbf{B}|^2}{4\pi} - \rho\left(\frac{v_A^2}{c^2} - \frac{v_A^4}{c^4}\right) |\mathbf{v}_\perp|^2 + \frac{v_A^2}{c} \left(\frac{m_i}{q_i} - \frac{m_e}{q_e}\right) \mathbf{v}_\perp \cdot \frac{\boldsymbol{\nabla} \times \mathbf{B}}{4\pi}\right] + \frac{c^2}{\omega_p^2}\frac{|\boldsymbol{\nabla} \times \mathbf{B}|^2}{4\pi}, \tag{40}$$

where v_A is the Alfven speed, $\mathbf{v}_\perp \doteq \mathsf{T} \cdot \mathbf{v}$ is the perpendicular velocity (to the magnetic field), $\mathsf{T} \doteq \mathbb{I}_3 - \mathbf{b} \otimes \mathbf{b}$ is a tensor, and $\mathbf{b} \doteq \mathbf{B}/|\mathbf{B}|$. It is worth mentioning that, in this theory, $(\rho, \mathbf{v}, \mathbf{B})$ are not exactly the ion mass density, ion velocity, and magnetic fields. Instead, they are transformed fields that are obtained using perturbative Lie transforms. As an example, here the mass density is given by $\rho = (1 + \nu Z_i) m_i n_i$ to lowest order. For the sake of conciseness, I shall not calculate explicitly the Frechet derivatives on the Hamiltonian appearing in Eqs. (39).

B. Linearized equations

As in the previous sections, we now linearize the extended-MHD equations (39). The linearized equations for the velocity and magnetic fields are

$$\frac{\partial \widetilde{\mathbf{u}}}{\partial t} = \frac{c}{4\pi\rho_0}(\boldsymbol{\nabla} \times \widetilde{\mathbf{B}}) \times \times \mathbf{B}_0 + \frac{c^2}{w_p^2}\frac{c}{4\pi\rho_0}\left\{\boldsymbol{\nabla} \times [\boldsymbol{\nabla} \times (\boldsymbol{\nabla} \times \widetilde{\mathbf{B}})]\right\}) \times \mathbf{B}_0, \tag{41a}$$

$$\begin{aligned}\frac{\partial \widetilde{\mathbf{B}}}{\partial t} &= -\boldsymbol{\nabla} \times [\mathbf{B}_0 \times (1 - \frac{v_A^2}{c^2}\mathsf{T} + \frac{v_A^4}{c^4}\mathsf{T}) \cdot \widetilde{\mathbf{u}}] + \frac{(1 - Z_i\nu)m_i}{q_e Z_i}\frac{v_A^2 c}{4\pi\rho_0}\,\boldsymbol{\nabla} \times \left\{\mathbf{B}_0 \times \mathsf{T} \cdot \boldsymbol{\nabla} \times \widetilde{\mathbf{B}}\right\} \\ &\quad - \left(\frac{|\mathbf{B}|}{\Omega_i} - \frac{|\mathbf{B}|}{\Omega_e}\right)\frac{c}{4\pi\rho_0}\boldsymbol{\nabla} \times [(\boldsymbol{\nabla} \times \widetilde{\mathbf{B}}) \times \mathbf{B}_0] - \left(\frac{|\mathbf{B}|}{\Omega_i} - \frac{|\mathbf{B}|}{\Omega_e}\right)\frac{c}{4\pi\rho_0}\frac{c^2}{\omega_p^2}\boldsymbol{\nabla} \times \left\{\boldsymbol{\nabla} \times [\boldsymbol{\nabla} \times (\boldsymbol{\nabla} \times \widetilde{\mathbf{B}})] \times \mathbf{B}_0\right\}.\end{aligned} \tag{41b}$$

Using the Fourier ansatz, these equations of motion are written as

$$\omega\widehat{\mathbf{u}} = \frac{v_A}{c}\mathbf{e}_z \times (\mathbf{k}c \times \widehat{\mathbf{B}}) - \frac{v_A}{c}\frac{1}{\omega_p^2}\mathbf{e}_z \times \left\{c\mathbf{k} \times [c\mathbf{k} \times (c\mathbf{k} \times \widehat{\mathbf{B}})]\right\}, \tag{42a}$$

$$\begin{aligned}\omega\widehat{\mathbf{B}} &= \frac{v_A}{c}\mathbf{k}c \times \left[\mathbf{e}_z \times \left(1 - \frac{v_A^2}{c^2}\mathsf{T} + \frac{v_A^4}{c^4}\mathsf{T}\right)\widehat{\mathbf{u}}\right] - \frac{v_A^4}{c^4}\left(\frac{1}{\Omega_i} - \frac{1}{\Omega_e}\right)\mathbf{k}c \times \left\{\mathbf{e} \times \mathsf{T} \cdot \mathbf{k}c \times \widehat{\mathbf{B}}\right\} \\ &\quad + i\left(\frac{1}{\Omega_i} - \frac{1}{\Omega_e}\right)\frac{v_A^2}{c^2}\mathbf{k}c \times [\mathbf{e_z} \times (\mathbf{k}c \times \widehat{\mathbf{B}})] \\ &\quad - i\left(\frac{1}{\Omega_i} - \frac{1}{\Omega_e}\right)\frac{v_A^2}{c^2}\frac{1}{w_p^2}\mathbf{k}c \times \left(\mathbf{e}_z \times \{\mathbf{k}c \times [\mathbf{k}c \times (\mathbf{k}c \times \widehat{\mathbf{B}})]\}\right).\end{aligned} \tag{42b}$$

C. Dispersion relation

We then adopt the same convention for the background magnetic field and the wave vector $\mathbf{k}$ that was used in the previous sections. When inserting Eqs. (42) into Mathematica, we obtain the eigenvalue equation $\boldsymbol{\mathcal{D}}\cdot\widehat{\mathbf{B}} = \mathcal{O}(\epsilon^3)$, where the dispersion tensor is given by

$$\boldsymbol{\mathcal{D}} \doteq \begin{pmatrix} \omega^2 - \frac{k_z^2 v_A^2}{1+v_A^2/c^2}\left(1+\frac{k^2c^2}{\omega_p^2}\right) & -i\frac{k_z^2 v_A^2}{1+v_A^2/c^2}\left(\frac{\omega}{\Omega_i}-\frac{\omega}{\Omega_e}\right)\left(1+\frac{k^2c^2}{\omega_p^2}\right) & \frac{k_x k_z v_A^2}{1+v_A^2/c^2}\left(1+\frac{k^2c^2}{\omega_p^2}\right) \\ i\frac{k_z^2 v_A^2}{1+v_A^2/c^2}\left(\frac{\omega}{\Omega_i}-\frac{\omega}{\Omega_e}\right)\left(1+\frac{k^2c^2}{\omega_p^2}\right) & \omega^2 - \frac{k_z^2 v_A^2}{1+v_A^2/c^2}\left(1+\frac{k^2c^2}{\omega_p^2}\right) & -i\frac{k_x k_z v_A^2}{1+v_A^2/c^2}\left(\frac{\omega}{\Omega_i}-\frac{\omega}{\Omega_e}\right)\left(1+\frac{k^2c^2}{\omega_p^2}\right) \\ \frac{k_x k_z v_A^2}{1+v_A^2/c^2}\left(1+\frac{k^2c^2}{\omega_p^2}\right) & i\frac{k_x k_z v_A^2}{1+v_A^2/c^2}\left(\frac{\omega}{\Omega_i}-\frac{\omega}{\Omega_e}\right)\left(1+\frac{k^2c^2}{\omega_p^2}\right) & \omega^2 - \frac{k_x^2 v_A^2}{1+v_A^2/c^2}\left(1+\frac{k^2c^2}{\omega_p^2}\right) \end{pmatrix}. \tag{43}$$

Calculating the determinant of $\boldsymbol{\mathcal{D}}$ and setting it to zero gives the dispersion relation for waves in extended-MHD:

$$\left[\omega^2 - \frac{k^2 v_A^2}{1+v_A^2/c^2}\left(1+\frac{k^2c^2}{\omega_p^2}\right)\right]\left[\omega^2 - \frac{k_z^2 v_A^2}{1+v_A^2/c^2}\left(1+\frac{k^2c^2}{\omega_p^2}\right)\right] - \left(\frac{k k_z v_A^2}{1+v_A^2/c^2}\right)^2\left(\frac{\omega}{\Omega_i}-\frac{\omega}{\Omega_e}\right)^2\left(1+\frac{k^2c^2}{\omega_p^2}\right)^2 = 0, \tag{44}$$

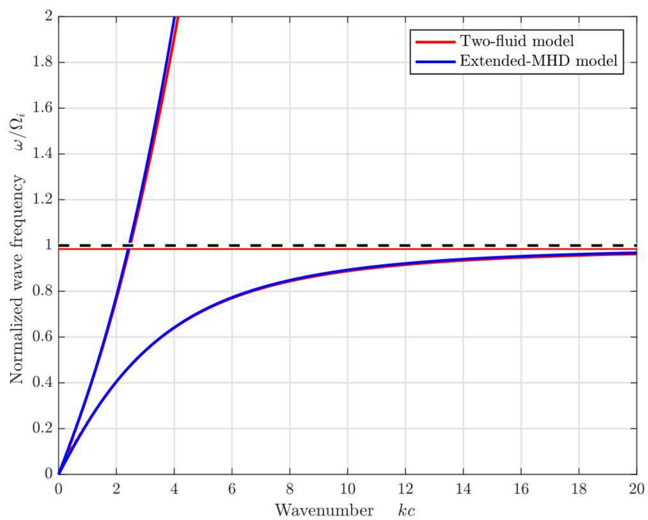

FIG. 4: Comparison of the normalized wave frequency ω/Ω_i using the extended-MHD and the two-fluid models. Good agreement is obtained for the shear Alfven wave.

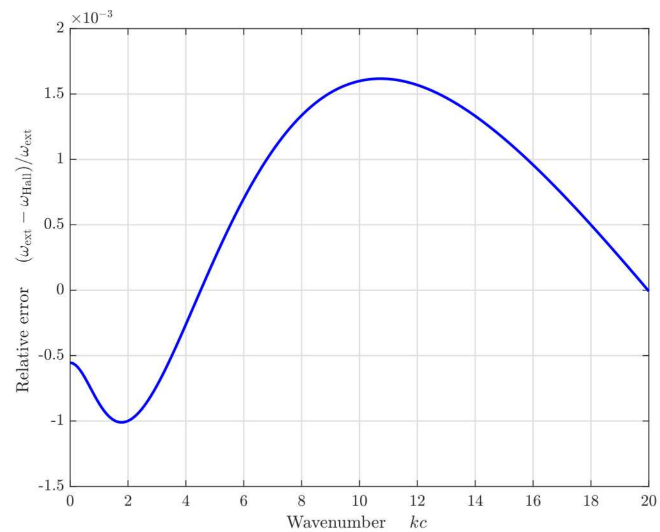

FIG. 5: Error between the dispersion curves obtained using Hall MHD and extended MHD for the shear Alfven wave.

where we avoiding writing the branch corresponding to $\omega = 0$.

Although the dispersion equation (44) might seem daunting, it is, in fact, quite similar to the dispersion equation (37) obtained using the Hall-MHD model. Specifically, we can interpret the new terms appearing in extended MHD as follows. The term

$$1 + \frac{k^2c^2}{\omega_p^2}$$

depends on the plasma frequency and can be associated to perturbative departures from exact charge neutrality. Also, the inverse of the ion gyrofrequency Ω_i appearing in the dispersion relation for Hall-MHD is replaced in extended-MHD by

$$\frac{1}{\Omega_i} - \frac{1}{\Omega_e}.$$

This term appears because extended MHD includes full effects of electron inertia. Finally, one can notice that the squared Alfven velocity v_A^2 in Hall MHD becomes

$$\frac{v_A^2}{1+v_A^2/c^2}$$

in extended MHD. This can be interpreted as a correction that is obtained when considering the speed of light finite, yet still large.

D. Comparison with two-fluid model

When comparing the extended-MHD waves with the waves in the two fluid model, one can see in Fig. 4 that the dispersion curves for the shear Alfven wave are almost identical. In fact, it seems that, for the shear Alfven wave, the extended-MHD model is given only very small

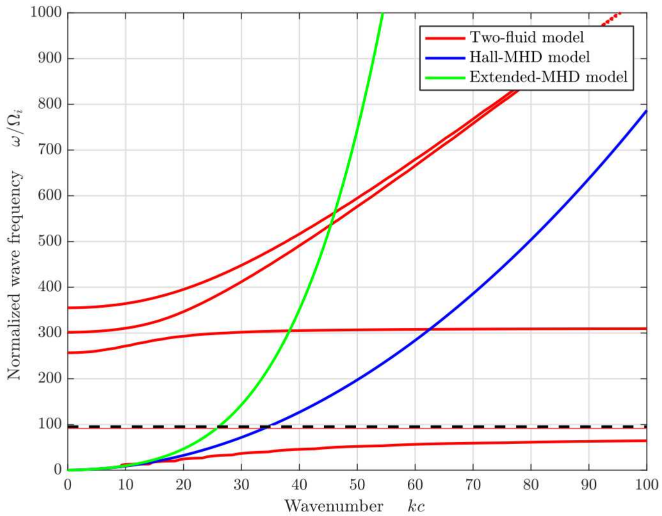

FIG. 6: Normalized wave frequency ω/Ω_i obtained using Hall-MHD, extended-MHD and the two-fluid models. At high wave numbers, both MHD models diverge, as expected.

corrections to the dispersion relation obtained using Hall MHD. In order to quantify this, Fig. 5 shows the relative error between the Hall-MHD and the extended-MHD frequencies. As shown, the relative error is of the order of 10^{-3}. Thus, for the parameter regime chosen in this work, extended-MHD does not give a significant correction to the dispersion curves for shear Alfven waves.

Regarding the compressional Alfven wave, just like in Hall MHD, the dispersion curves for extended-MHD also diverge for frequencies beyond the ion gyrofrequency. However, it is to be noted that, in Hall MHD, the frequency is proportional to k^2 in the limit of $k \to \infty$. In contrast, in extended MHD, the frequency diverges as k^4 in the limit of $k \to \infty$. This behavior is shown in Fig. 6.

VI. CONCLUSIONS

In this work, a study is presented comparing the dispersion relations for waves found in the ideal-, Hall-, and extended-MHD models. It is shown that, for frequencies below or close to the ion gyrofrequency, Hall MHD and extended MHD reproduce quite accurately the wave dispersion relations. For the parameter regime studied in this work, it seems that Hall MHD reproduces quite accurately the dispersion curves obtained using the more complicated extended-MHD model. However, at higher wave frequencies, both Hall- and extended-MHD models diverge from the dispersion curves obtained using the two-fluid model.

I would like to acknowledge fruitful discussions with D. E. Ruiz. This work was supported by the U.S. DOE through Contract DE-AC02-09CH11466 and by Sandia National Laboratories. Sandia National Laboratories is a multimission laboratory managed and operated by National Technology and Engineering Solutions of Sandia, LLC., a wholly owned subsidiary of Honeywell International, Inc., for the U.S. DOE National Nuclear Security Administration under contract DE-NA-0003525. This paper describes objective technical results and analysis. Any subjective views or opinions that might be expressed in the paper do not necessarily represent the views of the U.S. Department of Energy or the United States Government.

[1] J. P. Friedberg, *Ideal Magnetohydrodynamics* (Plenum Press, New York, 1987).
[2] T. J. Awe, R. D. McBride, C. A. Jennings, D. C. Lamppa, M. R. Martin, D. C. Rovang, S. A. Slutz, M. E. Cuneo, A. C. Owen, D. B. Sinars, et al., "Observations of modified three-dimensional instability structure for imploding z-pinch liners that are premagnetized with an axial field," Phys. Rev. Lett. **111**, 956 (2013).
[3] C. E. Seyler, M. R. Martin, and N. D. Hamlin, "Helical instability in MagLIF due to axial flux compression by low-density plasma," submitted.
[4] J. W. Burby, "Magnetohydrodynamic motion of a two-fluid plasma," Phys. Plasmas **24**, 082104 (2017).